ACS Synthetic Biology
Cite This: ACS Synth. Biol. 2019, 8, 297−306
Research Article
pubs.acs.org/synthbio

Development of a Synthetic 3-Dehydroshikimate Biosensor in *Escherichia coli* for Metabolite Monitoring and Genetic Screening

Liangpo Li,[†,‡] Ran Tu,[*,†] Guotian Song,[†,‡] Jie Cheng,[†,§] Wujiu Chen,[†] Lin Li,[†] Lixian Wang,[†] and Qinhong Wang[*,†]

[†]CAS Key Laboratory of Systems Microbial Biotechnology, Tianjin Institute of Industrial Biotechnology, Chinese Academy of Sciences, Tianjin 300308, People's Republic of China

[‡]University of the Chinese Academy of Sciences, Beijing, 100049, People's Republic of China

[§]Department of Chemical Engineering, School of Chemistry and Chemical Engineering, Chongqing University, Chongqing 401331, People's Republic of China

Supporting Information

ABSTRACT: Biosensors for target metabolites provide powerful high-throughput screening tools to obtain high-performing strains. However, well-characterized metabolite-sensing modules are often unavailable and limit rapid access to the robust biosensors with successful applications. In this study, we developed a strategy of transcriptome-assisted metabolite-sensing (TAMES) to identify the target metabolite-sensing module based on selectively comparative transcriptome analysis between the target metabolite producing and nonproducing strains and a subsequent quantative reverse transcription (RT-qPCR) evaluation. The strategy was applied to identify the sensing module *cusR* that responds positively to the metabolite 3-dehydroshikimate (DHS) and proved it was effective to narrow down the candidates. We further constructed the *cusR*-based synthetic biosensor and established the DHS biosensor-based high-throughput screening (HTS) platform to screen higher DHS-producing strains and successfully increased DHS production by more than 90%. This study demonstrated that the TAMES strategy was effective at exploiting the metabolite-sensing transcriptional regulator, and this could likely be extended to develop the biosensor-based HTS platforms for other molecules.

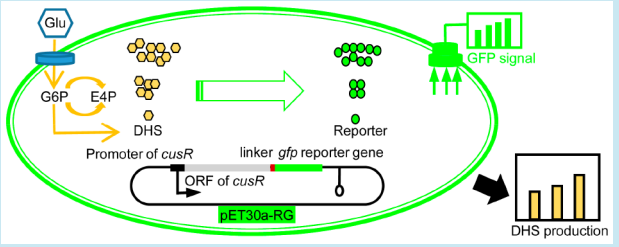

KEYWORDS: *biosensor, high-throughput screening, transcriptome analysis, metabolite-sensing module, transcriptional regulator, 3-dehydroshikimate*

The development of metabolic engineering resulted in an enormous increase in bioprocesses for the production of value-added compounds, such as amino acids, biofuels, organic acids, proteins, and polymers.[1] On the basis of renewable feedstocks, metabolic engineering approaches to design, construct, and modify the metabolic pathways and other cellular properties to produce various molecules (metabolites) of interest are of substantial economic and scientific interest.[2] However, the titer and yield of a final metabolite is often limited by the inefficient use of cellular resources and imbalanced metabolism.[3,4] Thus, reasonable and adequate metabolic regulation is essential to balance the metabolism and build efficient pathways to convert carbon sources to target metabolites. To achieve this goal, it is often indispensable to require cost-effective screening or selection methods to obtain the strain that produces the most effectively from a large number of possible combinations or a mutant library. Recent advances in synthetic biology, as well as modern high-throughput screening (HTS) technology (e.g., fluorescence-activated cell sorting), significantly contributed to the establishment of a novel tool for metabolic engineering: the synthetic biosensor,[4−6] which offers the potential to convert intracellular compound concentrations into measurable output and serves as an attractive tool for efficient screening. Many synthetic biosensors have been successfully constructed for HTS to improve the microbial production of a number of metabolites, including succinate, butanol, amino acids (e.g., L-tyrosine, L-leucine, L-arginine), and other high value-added molecules (e.g., flavonoids, lactam).[5,7−10]

The successful construction of synthetic biosensors requires effective, well-characterized metabolite-sensing modules, such as transcription factors, enzymes, periplasmic-binding proteins, riboswitches, and ribozymes to sense the intracellular or extracellular metabolites.[11,12] Thus, the identification of a target metabolite-sensing module is the key to constructing a robust synthetic biosensor. Researchers have exploited a number of mining strategies to identify suitable metabolite-sensing modules to develop novel biosensors: (1) those that are based on the biological databases to retrieve the target

Received: July 28, 2018
Published: January 4, 2019

DOI: 10.1021/acssynbio.8b00317
ACS Synth. Biol. 2019, 8, 297−306

metabolite-sensing modules to construct the corresponding biosensor (global databases, including RegPrecise,[13] DBD,[14] and PRODORIC,[15] are useful tools to gain information about prokaryotic regulons and transcription factors) and (2) those based on molecular shape and cheminformatic similarity algorithms to identify or design regulatory ligands and cognate transcription factor pairs, as well as fluorescence proteins, to construct the corresponding biosensor.[10] These strategies have greatly promoted the development and application of synthetic biosensors to monitor and screen metabolites. However, these strategies still have many limitations. For example, retrieving target metabolite-sensing modules primarily relies on the information on related metabolic pathways or regulatory circuits from databases. Designing regulatory ligand and cognate transcription factor pairs is not always successful. Therefore, it is critical to exploit new strategies to identify useful metabolite-sensing modules to construct a robust synthetic biosensor.

As the cost of DNA sequencing continues to decrease and the amount of sequence data generated grows, high-throughput sequencing technology, especially high-throughput transcriptome sequencing and analysis, plays an increasingly important role in identifying functional genes and biosynthetic pathways and analyzing the gene expression patterns.[16,17] Therefore, we developed a strategy to identify appropriate metabolite-sensing module candidates based on transcriptome sequencing and analysis, which was named the "transcriptome-assisted metabolite-sensing (TAMES)" strategy. This strategy follows two steps: (1) identify appropriate metabolite-sensing module candidates based on transcriptome sequencing and analysis and (2) confirm the target gene responding to the endogenous or exogenous target metabolite using quantitative reverse transcription PCR (RT-qPCR) technology. To verify the feasibility of the TAMES strategy, we applied it to discover a metabolite-sensing module for 3-dehydroshikimate (DHS), which is a critical intermediate of the shikimate and aromatic amino acid biosynthetic pathway in plants and microbes.[18,19] In addition, DHS is also an important precursor to synthesize a broad array of fine chemical products, such as protocatechuate, vanillin, catechol, adipate, and aspirin (acetylsalicylate).[20−23] In this study, we applied the TAMES strategy to explore the DHS-sensing transcriptional regulator gene and built a biosensor-based HTS platform to screen high performance strains for DHS production.

RESULTS

Screening and Identification of a Transcriptional Regulator for a Positive Response to DHS. Transcriptional regulators are one of the most common and valuable biosensor types developed for high-throughput screening.[5,11] In this study, we used the strategy of TAMES to search a DHS-sensing transcriptional regulator. At first, according to the first step of the TAMES strategy, we identified appropriate metabolite-sensing module candidates based on transcriptome sequencing and analysis. Cell samples of the DHS producer *E. coli* TIB02[24] at different fermentation times (TIB02-12h and TIB02-20h) were chosen as the test groups for transcriptome sequencing and analysis, while the cell sample of the non-DHS producer *E. coli* ATCC8739 (8739-12h) served as the control group. A total of 4199 genes successfully mapped to the *E. coli* ATCC8739 genome from these three groups of transcriptomes. The fragments per kilobase of exon per million fragments mapped (FPKM) value showed that a total of 527 genes were upregulated in the groups of the DHS producer (TIB02-12h and TIB02-20h) compared to that of the non-DHS producer (8739-12h; Table S1), and 19 genes were transcriptional regulators. Since transcriptional regulators can often natively react to stimuli such as small metabolites,[11] we analyzed the expression of 19 transcriptional regulators in more detail and fished out 10 transcriptional regulators with the following criteria: (1) 8739-12h_FPKM < TIB02-12h_FPKM < TIB02-20h_FPKM, (2) the gene transcriptional abundance in *E. coli* ATCC8739 should be as low as possible, and (3) the difference between TIB02-20h_FPKM and TIB02-12h_FPKM should be as high as possible (Table 1). To further identify the possibility that they functioned as DHS-sensing transcriptional regulators, these 10 candidates were verified at the transcriptional level by RT-qPCR with DHS either produced internally or added externally.

Table 1. FPKM Values of Potential DHS-Sensing Transcriptional Regulator Genes in Different Cell Samples Based on a Transcriptome Analysis

	FPKM value of cell samples		
gene	8739-12h	TIB02-12h	TIB02-20h
ypdB	7.73	91.88	227.83
yegW	13.02	18.28	40.59
yidZ	19.93	26.39	50.35
citB	28.78	49.17	93.30
narP	80.99	101.57	179.28
rcnR	59.04	107.14	187.17
cusR	14.32	25.70	44.68
cusS	55.96	58.82	78.57
bdcR	37.11	44.52	54.65
nadR	56.18	62.85	74.67

According to the second step of the TAMES strategy, we evaluated the candidates in response to endogenous or exogenous target metabolites using RT-qPCR. The transcription dynamic range of the DHS-sensing transcriptional regulator candidates was measured in two ways. First, the transcriptional expression levels of the candidates were measured at different fermentation times in the DHS-producing *E. coli* strain TIB02. The transcriptional expression levels of the genes *cusR* and *rcnR* increased with the production of DHS all the time (Figure 1A). The transcriptional expression level of the *cusR* gene changed approximately 3-fold, while the *rcnR* gene changed 2-fold. These results suggested that the *cusR* and *rcnR* genes could respond positively to the DHS produced—the endogenous target metabolite. With the exception of the *narp* and *bdcR* genes, the transcriptional expression levels of the other candidate genes increased in parallel with the fermentation time until 21 h, which was almost consistent with the results of the transcriptome analysis but decreased at 24 h. This implied that these genes should involve the complex response mechanism and not just respond because of the amount of DHS.

Then, the transcriptional expression levels of the selected candidates were also measured by adding different concentrations of exogenous DHS in NBS media in which the non-DHS producer *E. coli* ATCC8739 was grown. As the concentration of DHS (the exogenous target metabolite) increased from 0.5 g/L to 6.0 g/L, the transcriptional expression levels of the genes *cusR* and *bdcR* continually

DOI: 10.1021/acssynbio.8b00317
ACS Synth. Biol. 2019, 8, 297−306

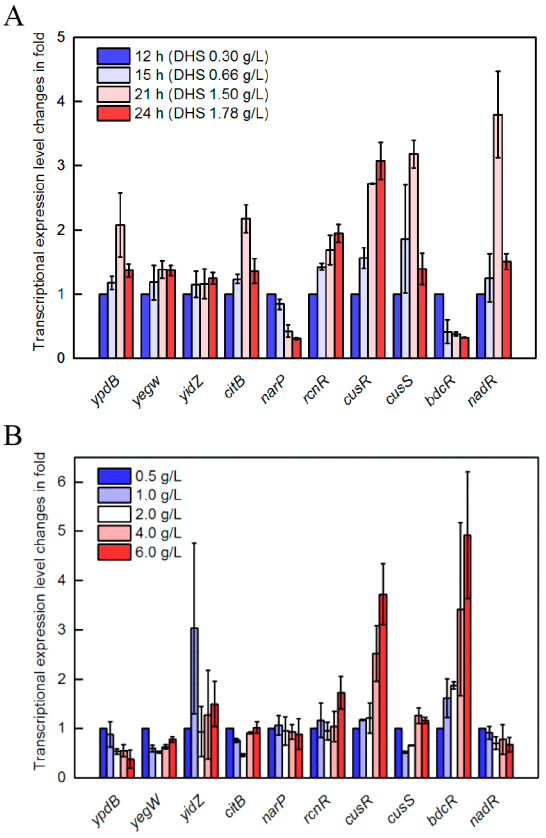

Figure 1. RT-qPCR analysis of the transcriptional expression level of potential transcriptional regulators to sense DHS. (A) Endogenous response analysis in DHS-producing *E. coli* strain TIB02 at different fermentation times. (B) Exogenous response analysis in the non-DHS-producing *E. coli* strain ATCC8739 supplemented with different concentrations of DHS. The plot is the average mean of triplicate samples, and the error bars represent standard deviations.

increased (Figure 1B). Under this dynamic transcription range, the maximum transcriptional expression levels of the *cusR* gene reached approximately 4-fold compared to that at the lowest DHS concentration, and the *bdcR* gene reached approximately 5-fold, while the other genes did not show a significant positive correlation. These results indicated that the transcriptional regulator genes *cusR* and *bdcR* have a positive response to the exogenous DHS. On the basis of the consistent response to either endogenous or exogenous DHS, the transcriptional regulator gene *cusR* had a stable positive response in both validations and was subsequently chosen to test the possibility of constructing the DHS biosensor.

Design and Construction of a Synthetic Biosensor to Monitor Exogenous and Endogenous DHS. Using transcriptome analysis and the RT-qPCR experiments (*in vitro* condition), the gene *cusR* was confirmed to positively respond to DHS in both exogenous and endogenous conditions, but we still lacked an understanding of the mechanism by which *cusR* responds to DHS. Therefore, we investigated how different versions of *cusR* and its cognate promoter affected the DHS response. The entire sensorR (pET30a-RG) was constructed by fusing the complete gene sequence of *cusR*, including the cognate promoter and the coding region of *cusR*, with the *gfp* reporter gene via a linker into a medium copy vector plasmid pET30a(+), and the promoter sensorRp (pET30a-RpG) was constructed by fusing the cognate promoter sequence of *cusR* with the *gfp* reporter gene into the vector plasmid (Figure S1A,B). The recombinant plasmids pET30a-RG or pET30a-RpG were then transformed into strains and their fluorescence intensities measured in the presence or absence of DHS. As shown in Figure 2, the DHS-

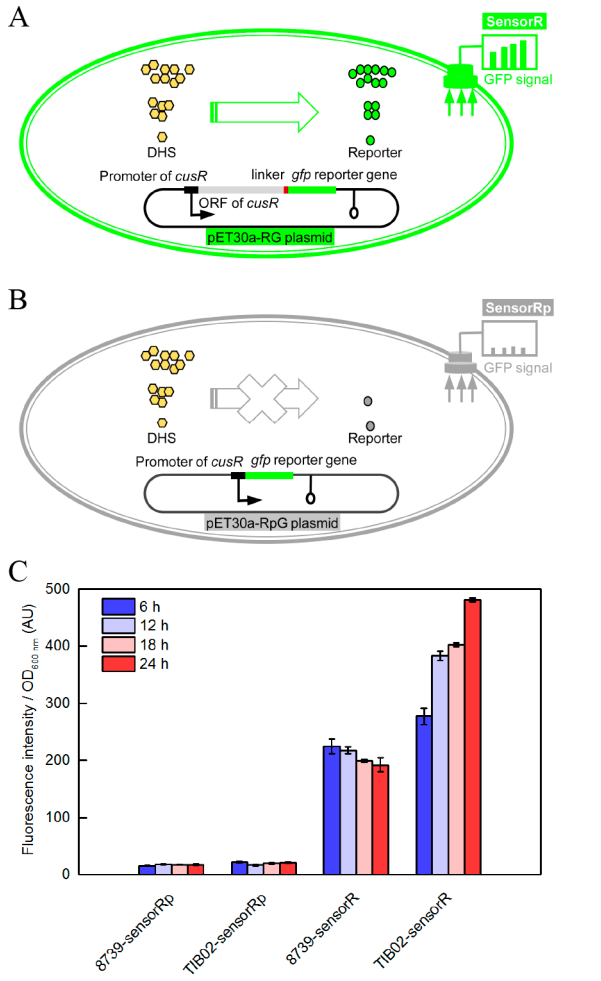

Figure 2. Construction and analysis of the genetically encoded biosensor. (A) Construction of sensorR using the plasmid pET30a-RG, including the complete *cusR* gene with the cognate promoter and the coding region of *cusR* and the reporter gene *gfp*. (B) Construction of sensorRp using the plasmid pET30a-RpG, including the cognate promoter part of *cusR* and the reporter gene *gfp*. (C) Endogenous response analysis of the candidates at different fermentation times. Sensor plasmids were constructed as described, transformed, and validated in the DHS-producing *E. coli* strain TIB02 and the non-DHS-producing *E. coli* strain ATCC8739 as the control. The plot is the average mean of triplicate samples, and the error bars represent standard deviations.

producing *E. coli* strain TIB02-sensorR had significantly increased fluorescence signals with the production of DHS, while the control strain 8739-sensorR lacked the increased fluorescence signals during the fermentation. At the same time, there were no obvious increases of fluorescent signals in the *E. coli* strain TIB02-sensorRp and 8739-sensorRp. These results indicated that it is the complete gene of *cusR* and not its cognate promoter required for responding to DHS (Figure 2).

We then constructed a series of promoter cutoff plasmids to investigate the effect of promoter length on the response ability to DHS. Different truncated promoters (0, 25, 50, 100 bp

DOI: 10.1021/acssynbio.8b00317
ACS Synth. Biol. 2019, 8, 297−306

length) together with the coding region of *cusR* and the *gfp* reporter gene were cloned into the vector pET30a(+) to generate pET30a-0-RG, pET30a-25-RG, pET30a-50-RG, and pET30a-100-RG, respectively (Figure S1C). As shown in Figure S2A, the DHS-producing *E. coli* strain TIB02 harboring pET30a-RG had the highest response signal compared to those truncated promoter variants. The truncated promoter variant pET30a-50-RG had a higher signal than the pET30a-100-RG or pET30a-25-RG, which might be due to self-regulation from its palindrome structure.[33] Interestingly, the fluorescent signal of TIB02 harboring pET30a-25-RG, which lacked the −10/35 motif, had a higher dynamic response range (about 6-fold change) than other truncated promoter sensors and the entire sensor pET30a-RG (about 2.6-fold change). The TIB02 harboring pET30a-0-RG, which lacked the full promoter part, had a higher signal than pET30a-0-RdelG, which had the first 4−30 nt of the *cusR* coding region deleted. There were no significant differences between pET30a-0-RdelG, pET30a-RdelG, and pET30a-RpG (Figure S2B). The results revealed there might be other cryptic promoters near the start codon and the first 4−30 nt of the coding region of *cusR* that are important for the biosensor. We also analyzed the direct interplay of CusR and DHS. Although the SDS-PAGE analysis showed that CusR could be induced by the exogenous DHS (Figure S3), an isothermal titration calorimetry (ITC) study showed that there was no binding interaction between DHS and CusR (Figure S4). On the basis of the above results, we used the entire sensorR for the subsequent study.

An ideal biosensor should have a number of good features: a wide dynamic range and strict specificity.[25] To validate that the biosensor can report quantitative and specific changes in DHS concentration. We determined the dose-dependent response curves to characterize the synthetic biosensor's dynamic range in either endogenous or exogenous DHS. To investigate the effect of endogenous DHS on the synthetic biosensor, the DHS-producing *E. coli* strain TIB02 harboring the sensorR plasmid was cultured and analyzed for the production of DHS. As shown in Figure 3A, the fluorescence signal increased as the production of DHS increased. After 24 h fermentation, the extracellular concentration of DHS was 1.8 g/L, and the fluorescence signal was 2.5-fold higher compared to that at 1 h. To investigate the effect of exogenous DHS on the synthetic biosensor, the non-DHS-producing strain *E. coli* ATCC8739 harboring the sensorR plasmid was cultivated to a logarithmic period of approximately 0.8 to 1.0 at OD_{600} in fermentation media where different concentrations of DHS from 0 to 6 g/L as inducers were added, and the fluorescence signals of the cells were measured after the addition of the exogenous DHS for 3 h. As shown in Figure 3B, the biosensor demonstrated a correlation of the fluorescence signal with the exogenous DHS concentration, and it had a 2.57-fold increased fluorescence signal when the high concentration of 6 g/L DHS was compared to the zero DHS condition. Those results implied that the biosensor could sense and respond to both endogenous and exogenous DHS in cells (*in vivo* analysis), which was consistent with the result of the transcriptome analysis and RT-qPCR verification (*in vitro* analysis). Therefore, this synthetic biosensor should have the potential to be an effective tool to monitor and screen strains for DHS production.

To further characterize the specificity of the synthetic DHS biosensor to other DHS structural analogues or DHS biosynthetic precursors/intermediates, the sensorR plasmid

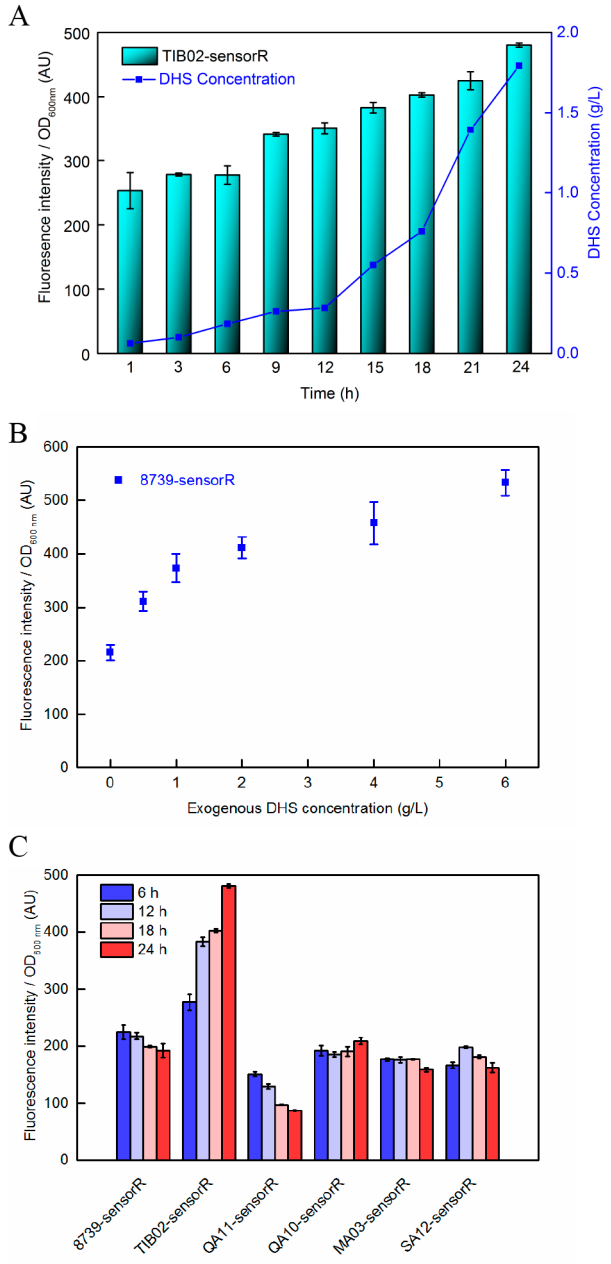

Figure 3. Characterization of the genetically encoded biosensors. (A) Exogenous response analysis using the non-DHS-producing *E. coli* strain ATCC8739 harboring sensorR plasmid pET30a-RG by supplementing different concentrations of DHS. (B) Endogenous response analysis using the DHS-producing *E. coli* strain TIB02 harboring sensorR plasmid pET30a-RG at different fermentation times. (C) Specificity of the response analysis using DHS structural analogues or biosynthetic precursor strains harboring the sensorR plasmid pET30a-RG. The plot is the average mean of triplicate samples, and the error bars represent standard deviations.

was transformed into strains constructed in a previous study (unpublished data): *E. coli* strain QA11 that produced 3-dehydroquinate (DHQ, a biosynthetic precursor of DHS), *E. coli* strain QA11 that produced quinate (a structural analogue of DHS), *E. coli* strain M that produced protocatechuate (a structural analogue of DHS), and *E. coli* strain SA12 that produced shikimate (a structural analogues of DHS), respectively (Figure S5). These strains could produce up to 1.5−3 g/L DHS structural analogues or DHS biosynthetic

DOI: 10.1021/acssynbio.8b00317
ACS Synth. Biol. 2019, 8, 297−306

precursors in shaking flasks and were compared with the DHS-producing strain *E. coli* TIB02 and the non-DHS-producing strain *E. coli* ATCC8739 harboring the sensor plasmid by measuring fluorescence intensities. Figure 3C showed the biosensor displayed excellent selectivity against the DHS structural analogues and its precursors or intermediates at 1.5−3 g/L. The fluorescence signals of *E. coli* QA11, QA10, MA03, and SA12 were similar to that of the control strain *E. coli* ATCC8739 and did not increase with the production of the corresponding chemicals, while the fluorescence signal of *E. coli* TIB02 with the sensor plasmid significantly increased following the formation of DHS. Thus, we demonstrated that the synthetic biosensor sensorR can specifically sense DHS and should be suitable for the high-throughput screening of overproducing DHS strains due to its excellent specificity, as well as its wide dynamic range.

Development and Application of a High-Throughput Screening Platform Based on a Genetically Encoded Biosensor for DHS Overproduction. Before utilizing the synthetic biosensor to screen the target strain mutant library, it is necessary to understand the performance of biosensors in the mutant strains. First, DHS-producing *E. coli* strain TIB02 harboring the sensorR plasmid pET30a-RG was moderately mutated with atmospheric and room temperature plasma (ARTP) to obtain a mutant library,[26] which has the highest positive mutation probability with a lethality between 90% and 95%. The lethality curve of the strains is shown in Figure S6. The mutant library was applied to produce DHS followed by the measurement of fluorescence intensities via fluorescence-activated cell sorting (FACS). The fluorescence signals of the mutant library gradually increased as the DHS was produced (Figure 4), and the greatest discrepancy of the fluorescence

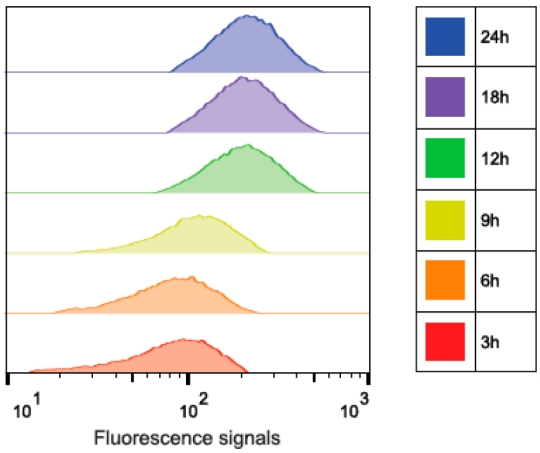

Figure 4. FACS analysis of fluorescence intensity changes in the DHS-producing *E. coli* TIB02 mutant library at different fermentation times. The mutant library was generated from the DHS-producing *E. coli* TIB02 harboring the sensorR plasmid pET30a-RG by moderate treatment with atmospheric and room temperature plasma (ARTP), and the mutant library was utilized for DHS production.

signals was observed between the 9 and 12 h fermentations. Therefore, this fermentative condition for DHS production was considered to demonstrate the most suitable sensitivity range of the biosensor and was subsequently chosen to establish the FACS-based screening platform.

Subsequently, we investigated the feasibility of the synthetic DHS biosensor for high-throughput screening. The DHS-producing *E. coli* TIB02 mutant library harboring the sensorR plasmid pET30a-RG with approximately 20 million mutants was utilized to produce DHS for 10 h to allow the accumulation of DHS and induce the formation of the fluorescence signal, and the 1000 cells which had the highest fluorescence signal were sorted using FACS. The sorted variants were cultivated to replicate the positive strains, and FACS sorting was conducted again to obtain the potential 1000 best mutants. Finally, 10 strains were selected randomly from the potential 1000 mutants to further evaluate their DHS production capacities. The best mutant *E. coli* strain of the 10 evaluated was M9 that produced 2.64 g/L at the shaking flask level, while its parent DHS-producing strain *E. coli* TIB02 produced 2.20 g/L DHS, and the DHS production increased approximately 20% (Figure 5A). The selected mutant strain *E. coli* M9 was utilized for a second round of high-throughput screening. The three *E. coli* mutants M3−7, M3−8, and M7−7 that produced more DHS than *E. coli* M9 were confirmed, and the most effective mutant, *E. coli* M3−8, from the second-round screening produced 2.86 g/L DHS in shaking flasks with an additional 10% increase in DHS production compared to *E. coli* M9, the best mutant from the first-round screening. The total increase of the mutant *E. coli* M3−8 in the DHS production was more than approximately 30% compared to that of the parent strain *E. coli* TIB02 at the shaking flask level (Figure 5A). DNA sequencing showed there were no mutations either in gene *cusR* or *gfp* in the sensor plasmid and verified the effectiveness of the developed screening strategy. We compared the DHS production of the mutants *E. coli* M3−8, M9, and the parent strain *E. coli* TIB02 in more detail using fed-batch fermentation. As shown in Figure 5B−D, the parent strain *E. coli* TIB02 could produce 19.02 g/L DHS at 38 h; the mutant *E. coli* M9 from the first-round screening could produce 27.22 g/L DHS at 38 h, and the mutant *E. coli* M3−8 from second-round screening could produce 36.72 g/L DHS at 38 h, while the cell growth of these three strains was similar during fed-batch fermentation. The most effective strain (*E. coli* M3−8) could produce more than 93% DHS compared to the parent strain *E. coli* TIB02 at the level of 5 L of fed-batch fermentation. The results suggest the high-throughput screening platform based on a genetically encoded biosensor could significantly facilitate the generation of DHS-overproducing strains.

DISCUSSION

Developing efficient high-producing strains is a time-consuming, expensive, and tedious process that is often limited due to the low throughput of analytical methods relative to the strain or variant generation. Fortunately, with the advent of synthetic biology, genetically encoded biosensors can be utilized to target high-producing strains using high-throughput screening.[3−5,11,12] However, due to the absence of a suitable biosensor for most valuable metabolites, the strategy to screen and identify the metabolite-sensing module for a biosensor is a critical necessity. Living organisms have naturally evolved a variety of metabolite-sensing modules, such as transcriptional regulators, enzymes, periplasmic binding proteins and RNAs. Transcriptional regulators have been demonstrated to be exceptionally valuable tools for metabolic engineering applications and the single cell analysis of production strains.[27−30] Therefore, in this study, we presented the potential of the TAMES strategy to identify the metabolite-sensing transcriptional regulators. By following the strategy of

DOI: 10.1021/acssynbio.8b00317
ACS Synth. Biol. 2019, 8, 297−306

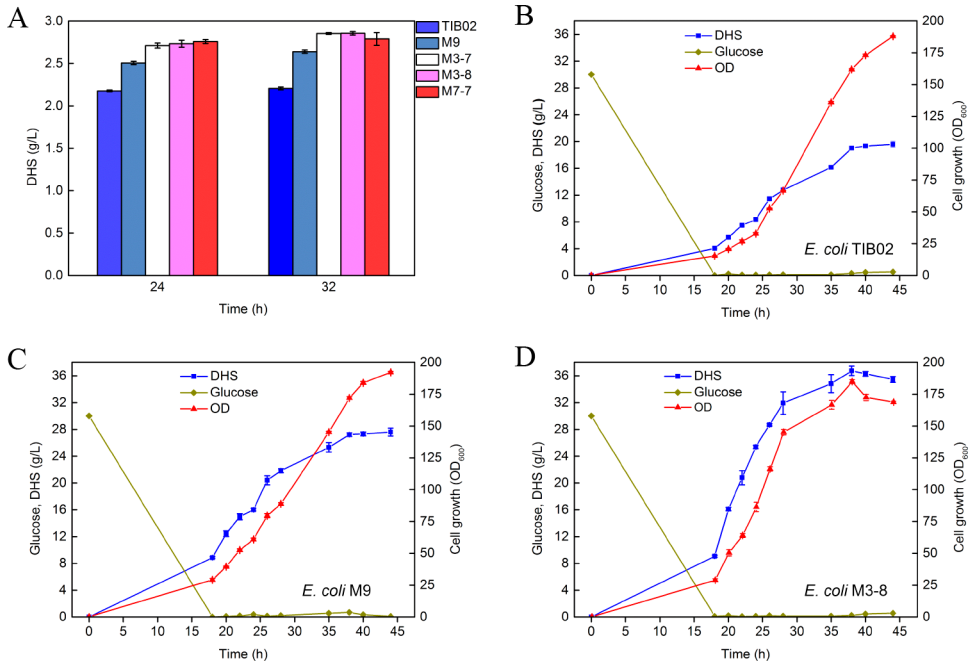

Figure 5. DHS production of the parent strain *E. coli* TIB02 and the mutants from DHS biosensor-based high-throughput screening. (A) DHS production in a 50 mL shaking flask. *E. coli* TIB02, the parent strain for DHS production; *E. coli* M9, the mutant from the first-round screening, and *E. coli* M3−7, M3−8, and M7−7, mutants from the second-round screening. (B) Fed-batch fermentation of the parent *E. coli* TIB02 for DHS production in a 5-L fermenter. (C) Fed-batch fermentation of the mutant *E. coli* M9 for DHS production in a 5-L fermenter. (D) Fed-batch fermentation of the mutant *E. coli* M3−8 for DHS production in a 5-L fermenter. Data are the average mean of triplicate samples, and the error bars represent standard deviations.

comparative transcriptome analysis between the target producing strain and the nontarget producing strain and a further RT-qPCR selection, we could easily narrow down the candidates (Table S1) and identify the effective target metabolite-sensing transcriptional regulator (CusR) to construct a biological encoded biosensor to monitor DHS production.

This biosensor architecture enables the intracellular detection of metabolite production by fusing reporters (e.g., fluorescent reporters, selection markers) to link the phenotype and genotype and convert metabolite production into a measurable output. The transcriptional regulator could directly control the expression of the reporter gene by linking the reporter gene to the downstream of the regulated gene promoter or by fusing the reporter gene with the regulated gene.[31,32] Our results showed the complete gene of *cusR*, including its cognate promoter, was required to synthesize an effective synthetic biosensor (Figure 2). A further promoter cutoff experiment showed that the *cusR* expression might be self-regulated by interactions with the single palindrome site upon its cognate promoter and that there could be additional cryptic promoters.[33] Promoter predictions on the BDGP Web site[34] indicated there were three additional cryptic promoters near the start codon. Two of them (GTG as the start codon in-frame) overlapped on the first 4−12 nt of the *cusR* coding region, which is consistent with the results that deleting the region 4−30 nt of the CusR disrupted the DHS sensing (Figure S2B). The literature reported that the gene *cusR* belongs to a two-component system together with the gene *cusS*, a histidine kinase. The CusR could be phosphorylated by CusS, and the phosphorylated CusR acts as an activator to further promote the two-component system.[33,35,36] However, deletion of either *cusS* or *cusR* in the genome did not affect the functions of the DHS biosensor, implying that the biosensor did not use a two-component system (Figure S2C). In addition, there was no binding interaction between DHS and CusR in our ITC analysis. Therefore, the mechanism of DHS sensing is still unclear and will be explored in the future.

The screening and analysis of bacterial cells tailored for metabolite production using a biosensor requires that the characteristics of the biosensor are well understood, such as its dynamic range, specificity, and sensitivity interval. In this study, our synthetic biosensor had a detection signal that corresponded to its RT-qPCR identification signal. The correlation observed between the fluorescence signals of the cells and the DHS concentrations indicated that this biosensor could be a potential tool for *in vivo* high-throughput screening (Figure 3). Figure S2D showed the dynamic range was lower in the presence of exogenous DHS. This might be due to inefficient transport across the cell membrane, causing a lower intracellular DHS concentration than what is added to the media. The specificity experiment showed that the biosensor displayed selectivity against all DHS biosynthetic precursors or structural analogues, including 3-dehydroquinate, quinate, protocatechuate, and shikimate (Figure 3C). This feature of the biosensor is useful to exclude the interference of other structural analogues when screening target phenotypes. For the sensitive interval, the sensor should respond strongly to the target metabolite, so that the response could be easily detected. On the basis of the analysis of the FACS, the biosensor was investigated for the screening time points between 9 and 12 h in which both the parent *E. coli* strain TIB02 (Figure S7) and the *E. coli* TIB02 mutant library (Figure 4) showed the most effective sensitive interval. The outcomes of the screening were often influenced by several factors, such as the original strain used for mutagenesis, the cultivation conditions, and the gating

DOI: 10.1021/acssynbio.8b00317
ACS Synth. Biol. 2019, 8, 297−306

strategy used in FACS,[37] which could be offset by the optimized screening time points with a better sensitivity for the biosensor. Therefore, the optimized screening parameter would be beneficial to improve the screening rate of the positive clones. Overall, our biosensor was successfully utilized to enrich the mutants with improved DHS production, and the mutant had a titer of DHS that was more than 90% higher than the original strain. Our study suggested that the synthetic biosensor could be applied to screen DHS-producing mutants using high-throughput screening.

CONCLUSION

In this study, we developed a TAMES strategy, which is based on transcriptome sequencing and analysis to discover a metabolite-sensing module and successfully found that the transcriptional regulator gene *cusR* including its cognate promoter was necessary to sensing the important metabolite DHS. We used the *cusR* and its cognate promoter and *gfp* reporter gene to construct a synthetic biosensor and demonstrated the GFP signal response to both intracellular and extracellular DHS. In addition, we established the DHS biosensor-based HTS and applied it to evolve and screen high-yield DHS-producing strains and obtained the improved mutant with a significant increase in DHS production. Our study demonstrated that the TAMES strategy could be a powerful tool to exploit the metabolite-sensing transcriptional regulators and could likely be extended to develop the biosensor-based HTS models to breed high-performance strains for the microbial production of many other molecules.

METHODS

Bacterial Strains, Media, and Growth and Fermentation Conditions. The bacterial strains and plasmids are listed in Table S2. Unless stated otherwise, the cells were routinely cultured using Luria−Bertani (LB) media at 37 °C. Cells for the transcriptome analyses, RT-qPCR verification, FACS screening, and fermentation evaluation were cultured with the fermentation medium (NBS) in a shaking flask at 37 °C, and 0.1 optical density (OD_{600}) of overnight LB culture was used as the seed culture. The fermentation medium (NBS) for the shaking flask contained KH_2PO_4, 3.5 g/L; $K_2HPO_4{\cdot}3H_2O$, 6.5 g/L; $(NH_4)_2HPO_4$, 3.5 g/L; $MgSO_4$, 0.120 g/L; $CaCl_2$, 11 mg/L; thiamine HCl, 5 mg/L; $FeCl_3{\cdot}6H_2O$, 0.16 mg/L; $CoCl_2{\cdot}6H_2O$, 0.2 mg/L; $CuSO_4{\cdot}5H_2O$, 0.015 mg/L; $ZnCl_2$, 0.02 mg/L; $Na_2MoO_4{\cdot}2H_2O$, 0.02 mg/L; and H_3BO_3, 0.005 mg/L. Depending on the resistance of strains, kanamycin was added at a final concentration of 25 mg/L, or ampicillin was added at a final concentration of 50 mg/L. The agar plates were incubated at 37 °C for 24 h. Fed-fermentation in a 5-L jar fermenter (Shanghai BaoXing Bioengineering Equipment Co, Ltd., China) was conducted as follows: Seeds were prepared as two successive precultures. The first culture was grown with LB media, and the second culture was grown with NBS media, respectively. After the second preculture grew to an OD_{600} of approximately 6, 200 mL of the second seed culture was transferred to the 5-L jar fermenter containing 1800 mL of the basal fermentation medium. The basal fermentation medium was comprised as follows: glucose, 30 g/L; $K_2HPO_4{\cdot}3H_2O$, 7.5 g/L; $(NH_4)_2SO_4$, 1.6 g/L; $MgSO_4{\cdot}7H_2O$, 2.0 g/L; citric acid, 2 g/L; $FeSO_4{\cdot}7H_2O$, 0.0075 g/L; $CoCl_2{\cdot}6H_2O$, 0.004 g/L; $ZnSO_4$, 0.0064 g/L; Na_2SO_4, 0.02 g/L; $Cu_2SO_4{\cdot}5H_2O$, 0.0006 g/L; and $MnSO_4{\cdot}H_2O$ 0.004525 g/L. Fed-batch fermentation was conducted at 37 °C, pH 7.0, and dissolved oxygen 10% or higher. The concentration of glucose was monitored using HPLC analysis (see the section of Metabolite Analysis) during the fermentation process to ensure the glucose concentration was maintained under 1 g/L.

DNA Manipulation. Strains with *cusR or cusS* deletions in their genomes were constructed using a modified method to delete *E. coli* chromosomal genes via two steps of homologous recombination.[38] Standard methods including the polymerase chain reaction (PCR), DNA restriction enzyme digestion, and ligation were conducted using standard protocols.[39] The relevant primers are listed in Table S3. To construct the plasmid pET30a-RG, the gene *cusR* without a stop codon was amplified using the genome of *E. coli* ATCC8739 as a template with the oligonucleotides cusR-F and cusR-R. The gene *gfp* without a start codon was amplified using the vector pET30a-GFP as a template with the oligonucleotides GFP-F and GFP-R. Overlap PCR was conducted with the oligonucleotides cusR-F and GFP-R using the amplified products containing the gene *cusR*, a linker (45 bp sequence from 5 to 3 direction: ggtggtggtggttctggtggtggtggatccggtggcggtggttct), and *gfp* as templates. The overlap PCR product was digested using *EcoR* I and *Hind* III and cloned into the vector pET30a(+) to obtain the recombinant plasmid pET30a-RG (Figure S1A), including the complete gene *cusR* and the green fluorescent gene *gfp*. To construct the plasmid pET30a-RpG (Figure S1B), the target PCR product was amplified from the plasmid pET30a-RG by PCR using the primer oligonucleotides cusRp-F and cusRp-R and ligated to form the plasmid pET30a-pRpG, including a fusion expression unit of the promoter of the *cusR* promoter and the green fluorescent gene *gfp*. To construct the plasmid pET30a-RdelG (Figure S1C), the target PCR product was amplified from the plasmid pET30a-RG by PCR using the primer oligonucleotides cusRdel-F and cusRdel-R and ligated to form the plasmid pET30a-pRdelG including a fusion expression unit of the cognate promoter of *cusR*, the coding region of *cusR* without the first 4−30 nt, and the green fluorescent gene *gfp*. To construct the promoter cutoff plasmids (Figure S1D), the target PCR product was amplified from the plasmid pET30a-RG by inverse PCR using forward primers 25-cusR-F, 50-cusR-F, and 100-cusR-F and reverse primer cutoff-cusR-R and ligated to form the plasmids pET30a-25-RG, pET30a-50-RG, and pET30a-100-RG, respectively. The target PCR product was amplified from the plasmid pET30a-RG by inverse PCR using the primers pET30a-0-RG-F, pET30a-0-RG-R, pET30a-R-F, and pET30a-R-R and ligated to form plasmids pET30a-0-RG and pET30a-R, respectively. The target PCR product was amplified from the plasmid pET30a-RdelG using the primers pET30a-0-RdelG-F and pET30a-0-RdelG-R and ligated to form the plasmid pET30a-0-RdelG.

Transcriptome Analysis. DHS-producing *E. coli* strain TIB02 and non-DHS-producing *E. coli* ATCC8739 were cultivated in NBS media, and *E. coli* ATCC8739 was sampled at 12 h (8739-12h), while *E. coli* TIB02 was sampled at 12 and 20 h, respectively (TIB02-12h and TIB02-20h). The cells were harvested by centrifugation at 5000*g* at 4 °C for 5 min, and the cell pellets were instantly frozen using liquid nitrogen and stored at −80 °C until RNA extraction.

The total RNA was extracted using an RNAiso Plus Kit (TAKARA, China). The RNA quantity was measured using a NanoDrop Spectrophotometer ND-2000 (Thermo Fisher Scientific, USA), and the RNA quality was assessed using an

DOI: 10.1021/acssynbio.8b00317
ACS Synth. Biol. 2019, 8, 297−306

Agilent 2100 Bioanalyzer (Agilent Technologies, USA). The cDNA libraries were prepared using a TruSeq Stranded Total RNA Library Prep Kit (Illumina, USA), and the Illumina sequencing was performed by GENEWIZ Inc. (China) using the Illumina HiSeq 2000 platform. Briefly, the mRNA was purified, fragmented, and primed for cDNA synthesis. The first strand cDNA was synthesized by priming RNA fragments using a random hexamer primer and transcribing reverse transcriptase. The second strand cDNA synthesis was subsequently conducted using first strand cDNA as the template with DNA polymerase I and RNase H. The cDNA was subjected to an end repair process, adenylation of the 3′ ends, and subsequent ligation of the adapter. Finally, the adaptor-ligated libraries were purified and enriched with PCR to create the final cDNA library. The quantified and qualified libraries were then sequenced.

After Illumina Hiseq2500 paired-end sequencing, the transcriptome data with a length of 101 bp were generated. The raw data from three cell samples were analyzed using Fast QC for quality assessment and preprocessed to get the clean data by removing low quality sequences and adaptors. The Q20, Q30, and GC contents of the clean data were calculated. The clean data of the three samples were mapped to the *E. coli* ATCC8739 genomes and the *E. coli* ATCC8739 genes by Bowtie2 (2.1.0). The *E. coli* ATCC8739 genome and genes file were downloaded from the NCBI (ftp://ftp.ncbi.nlm.nih.gov/genomes/archive/old_refseq/Bacteria/Escherichia_coli_ATCC_8739_uid58783/NC_010468.fna and ftp://ftp.ncbi.nlm.nih.gov/genomes/archive/old_refseq/Bacteria/Escherichia_coli_ATCC_8739_uid58783/NC_010468.ffn). To compare the transcriptional abundance of each sample, the fragments per kilobase of the exon model per million mapped reads were calculated for each gene based on the length of the gene and the number of reads mapped to the gene using the RSEM software (V 1.2.4).[40,41]

RT-qPCR Analysis. Total RNA was extracted using QuantiTect (Macherey−Nagel, Germany) according to the manufacturer's instructions. The samples were treated with DNase. The total RNAs were evaluated quantitatively and qualitatively using a NanoDrop ND-2000 spectrophotometer (Thermo Fisher Scientific, Wilmington DE, USA), and the RNA content was determined by measuring the absorption at 260 nm. The optimal purity of the RNA was ensured by determining the 260/280 adsorption ratio (values >2.00). The integrity of the extracted RNA was determined using gel electrophoresis with a 1.0% agarose gel stained with ethidium bromide and visualized under ultraviolet (UV) light. The cDNA synthesis reaction was performed in a total volume of 20 μL using a QuantiTect Reverse Transcription Kit (QIAGEN, Germany), and up to 2 μg RNA was used for the reverse transcription (RT) reaction following the manufacturer's instructions for the RNase treatment. The cDNA was conserved at −80 °C. The specificity validation of all the primers used in RT-qPCR was tested in *silico* using BLAST analysis. A description of the primer and gene is shown in Table S4. Real-time PCR was performed in 96-well plates on a fluorescence quantitative PCR instrument (Bio-Rad, USA) using SYBR Green as the fluorophore. The RT-qPCR mixes were prepared using iQ SYBR Green Supermix according to the manufacturer's instructions (Bio-Rad, USA). The PCR reactions were conducted in 20 μL volumes, which contained 10 μL of 2 × iQTM SYBR Green Supermix, 8 μL of template, 0.5 μL of forward and reverse primers (for each primer), and 1 μL of ddH_2O. Three replicates were included for each sample, and the 16s RNA gene was used as an internal control to normalize gene expression. The program for RT-qPCR was subjected to the following conditions: 95 °C for 3 min, 40 cycles of 95 °C for 15 s, 55 °C for 15 s, and 72 °C for 30 s. Dissociation curves with 0.3°C/s melt rates were conducted to check for the presence of nonspecific dsDNA SYBR Green hybrids. Only primers with a single PCR amplification product were used in the subsequent analyses. The amplification efficiency of each primer was calculated from the slope of the standard curve.[42] The relative expression levels were calculated using the $2^{-\triangle\triangle CT}$ method.[43]

Determination of Cell Growth and Fluorescence. The fluorescence and optical density of cell growth (OD_{600}) were determined using a SpectraMax M2e microplate reader (Molecular Devices, USA). The GFP fluorescence signal was measured with excitation at 480 nm and emission at 520 nm. The specific fluorescence was defined as the fluorescence per OD_{600} value (given in AU).

Mutagenesis and Library Screening. DHS-producing *E. coli* TIB02 carrying pET30a-RG was grown to the logarithmic period in LB media containing 25 μg/mL kanamycin, and the cells were harvested, washed, and resuspended in 1 mL of NaCl, 0.9% (w/v) at an OD_{600} of 1.0. Ten microliters of the cells were removed and spread on a 1 cm diameter metal plate. This plate was later exposed to the ARTP system's nozzle exit (ARTP-II, Beijing, China). The cell suspension was treated with an ARTP mutagenesis system for 15 s following the manual's instruction. Parameters such as Pin, Pout, and the distance (D) between the plasma torch nozzle exit and the sample plate, were set to 120 W (Pin), 20 W (Pout), and 2 mm (D). The flow rate of the helium gas was 10 L/min. After mutation, the plate was placed in a new sterile tube containing 990 μL of LB medium. The treated cells were regenerated in LB media for 3 h at 37 °C and inoculated into 50 mL of shaking flasks containing 10 mL of fermentation medium. Cultivation was performed at 37 °C and 220 rpm for 10 h. To screen for FACS, the cells were harvested, washed, and resuspended in phosphate buffer saline (PBS) with an OD_{600} of 1.0. The fluorescence signal in each cell was analyzed using FACS (MoFlo XDP, Beckman Coulter, USA) with the following parameters: excitation at 488 nm, detection fluorescence at 520 nm. The data were analyzed using the Beckman Summit software v5.2. On the basis of the preanalysis of the mutant library, the selection gate was set as 0.05% of the total cells. Finally, a total of 1000 cells were collected in fresh 500 μL of LB media from 2×10^6 cells using FACS, and the selected cells were spread on agar plates for overnight cultivation. Colonies that grew were cultivated for additional fermentation evaluation.

Metabolite Analysis. The production of DHS and the consumption of glucose in the *E. coli* strains were analyzed and quantified using high-performance liquid chromatography equipped with an Innoval C18 column (4.6 mm by 250 mm, 5 μm particle size) connected to a UV detector. The ratio of the phase A phosphoric acid 0.1% (W/W) was 80%, and the phase B methanol was 20%, respectively. The flow rate was 0.8 mL/min. The column temperature was 30 °C, and the eluent was monitored at a wavelength of 260 nm. The samples were centrifuged at 10 000*g* for 10 min. Each supernatant was diluted with 10 volumes of ddH_2O, and 20 μL of the diluted sample was injected. The calibration curves of pure DHS and

DOI: 10.1021/acssynbio.8b00317
ACS Synth. Biol. 2019, 8, 297−306

glucose were used to quantify the standard curves that were linear over the range of 0−10 mM (R^2 = 0.9992).

■ ASSOCIATED CONTENT

Supporting Information

The Supporting Information is available free of charge on the ACS Publications website at DOI: 10.1021/acssynbio.8b00317.

Supporting Tables S1−S4 and Figures S1−S7, supplementary methods including purification and SDS-PAGE analysis of CusR, and isothermal titration calorimetry (ITC) studies on the binding of DHS to CusR (PDF)

■ AUTHOR INFORMATION

Corresponding Authors

*Address: Tianjin Institute of Industrial Biotechnology, Chinese Academy of Sciences, 32 XiQiDao, Tianjin Airport Economic Area, Tianjin 300308, P.R. China. Tel.: +86-22-24828705. E-mail: tu_r@tib.cas.cn.

*Address: Tianjin Institute of Industrial Biotechnology, Chinese Academy of Sciences, 32 XiQiDao, Tianjin Airport Economic Area, Tianjin 300308, P.R. China. Tel.: +86-22-84861950. E-mail: wang_qh@tib.cas.cn.

ORCID

Qinhong Wang: 0000-0003-0004-2721

Author Contributions

L.L., R.T., and Q.W. designed the study, analyzed the data, and wrote the manuscript. L.L., G.S., J.C., L.L., W.C., and L.W. performed the experiments. All authors read and approved the final manuscript.

Notes

The authors declare no competing financial interest.

■ ACKNOWLEDGMENTS

This study was supported by the Science and Technology Service Network Initiative of the Chinese Academy of Sciences (KFJ-SW-STS-165), the Science and Technology Support Program of Tianjin, China (14ZCZDSY00066, 15PTCYSY00020), the Key Research Program of the Chinese Academy of Sciences (KFZD-SW-212-3-1), and the National Major Scientific and Technological Special Project of China (2017ZX09101003). R.T. was supported by the Youth Innovation Promotion Association of the Chinese Academy of Sciences (2012144).

■ REFERENCES

(1) Chae, T. U., Choi, S. Y., Kim, J. W., Ko, Y. S., and Lee, S. Y. (2017) Recent advances in systems metabolic engineering tools and strategies. *Curr. Opin. Biotechnol. 47*, 67−82.

(2) Keasling, J. D. (2010) Manufacturing molecules through metabolic engineering. *Science 330*, 1355−1358.

(3) Dietrich, J. A., McKee, A. E., and Keasling, J. D. (2010) High-throughput metabolic engineering: advances in small-molecule screening and selection. *Annu. Rev. Biochem. 79*, 563−90.

(4) Zhang, F., and Keasling, J. D. (2011) Biosensors and their applications in microbial metabolic engineering. *Trends Microbiol. 19*, 323−9.

(5) Mahr, R., and Frunzke, J. (2016) Transcription factor-based biosensors in biotechnology: current state and future prospects. *Appl. Microbiol. Biotechnol. 100*, 79−90.

(6) Ng, C. Y., Khodayari, A., Chowdhury, A., and Maranas, C. D. (2015) Advances in de novo strain design using integrated systems and synthetic biology tools. *Curr. Opin. Chem. Biol. 28*, 105−114.

(7) Binder, S., Siedler, S., Marienhagen, J., Bott, M., and Eggeling, L. (2013) Recombineering in *Corynebacterium glutamicum* combined with optical nanosensors: a general strategy for fast producer strain generation. *Nucleic Acids Res. 41*, 6360−6369.

(8) Chou, H. H., and Keasling, J. D. (2013) Programming adaptive control to evolve increased metabolite production. *Nat. Commun. 4*, 2595−2602.

(9) Siedler, S., Stahlhut, S. G., Malla, S., Maury, J., and Neves, A. R. (2014) Novel biosensors based on flavonoid-responsive transcriptional regulators introduced into *Escherichia coli*. *Metab. Eng. 21*, 2−8.

(10) Zhang, J., Barajas, J. F., Burdu, M., Ruegg, T. L., Dias, B., and Keasling, J. D. (2017) Development of a transcription factor-based lactam biosensor. *ACS Synth. Biol. 6*, 439−445.

(11) Lin, J. L., Wagner, J. M., and Alper, H. S. (2017) Enabling tools for high-throughput detection of metabolites: Metabolic engineering and directed evolution applications. *Biotechnol. Adv. 35*, 950−970.

(12) Liu, Y., Liu, Y., and Wang, M. (2017) Design, optimization and application of small molecule biosensor in metabolic engineering. *Front. Microbiol. 8*, 2012.

(13) Novichkov, P. S., Kazakov, A. E., Ravcheev, D. A., Leyn, S. A., Kovaleva, G. Y., Sutormin, R. A., Kazanov, M. D., Riehl, W., Arkin, A. P., Dubchak, I., and Rodionov, D. A. (2013) RegPrecise 3.0–a resource for genome-scale exploration of transcriptional regulation in bacteria. *BMC Genomics 14*, 745.

(14) Wilson, D., Charoensawan, V., Kummerfeld, S. K., and Teichmann, S. A. (2008) DBD–taxonomically broad transcription factor predictions: new content and functionality. *Nucleic Acids Res. 36*, D88−92.

(15) Münch, R., Hiller, K., Barg, H., Heldt, D., Linz, S., Wingender, E., and Jahn, D. (2003) PRODORIC: prokaryotic database of gene regulation. *Nucleic Acids Res. 31*, 266−269.

(16) Shendure, J., Balasubramanian, S., Church, G. M., Gilbert, W., Rogers, J., Schloss, J. A., and Waterston, R. H. (2017) DNA sequencing at 40: past, present and future. *Nature 550*, 345−353.

(17) Koboldt, D. C., Steinberg, K. M., Larson, D. E., Wilson, R. K., and Mardis, E. R. (2013) The next-generation sequencing revolution and its impact on genomics. *Cell 155*, 27−38.

(18) Maeda, H., and Dudareva, N. (2012) The shikimate pathway and aromatic amino Acid biosynthesis in plants. *Annu. Rev. Plant Biol. 63*, 73−105.

(19) Noda, S., and Kondo, A. (2017) Recent advances in microbial production of aromatic chemicals and derivatives. *Trends Biotechnol. 35*, 785−796.

(20) Li, K., and Frost, J. W. (1998) Synthesis of vanillin from glucose. *J. Am. Chem. Soc. 120*, 10545−10546.

(21) Draths, K. M., and Frost, J. W. (1995) Environmentally compatible synthesis of catechol from D-glucose. *J. Am. Chem. Soc. 117*, 2395−2400.

(22) Lin, Y., Sun, X., Yuan, Q., and Yan, Y. (2014) Extending shikimate pathway for the production of muconic acid and its precursor salicylic acid in *Escherichia coli*. *Metab. Eng. 23*, 62−69.

(23) Noda, S., Shirai, T., Oyama, S., and Kondo, A. (2016) Metabolic design of a platform *Escherichia coli* strain producing various chorismate derivatives. *Metab. Eng. 33*, 119−129.

(24) Li, Z., Li, Y., Chen, W., Cao, Q., Guo, Y., Wan, N., Jiang, X., Tang, Y. J., Wang, Q., and Shui, W. (2017) Integrating MS1 and MS2 scans in high-resolution parallel reaction monitoring assays for targeted metabolite quantification and dynamic 13C-labeling metabolism analysis. *Anal. Chem. 89*, 877−885.

(25) Fang, M., Wang, T., Zhang, C., Bai, J., Zheng, X., Zhao, X., Lou, C., and Xing, X. H. (2016) Intermediate-sensor assisted push-pull strategy and its application in heterologous deoxyviolacein production in *Escherichia coli*. *Metab. Eng. 33*, 41−51.

(26) Zhang, X., Zhang, X. F., Li, H. P., Wang, L. Y., Zhang, C., Xing, X. H., and Bao, C. Y. (2014) Atmospheric and room temperature plasma (ARTP) as a new powerful mutagenesis tool. *Appl. Microbiol. Biotechnol. 98*, 5387−96.

(27) Liu, D., Evans, T., and Zhang, F. (2015) Applications and advances of metabolite biosensors for metabolic engineering. *Metab. Eng. 31*, 35−43.
(28) Michener, J. K., Thodey, K., Liang, J. C., and Smolke, C. D. (2012) Applications of genetically-encoded biosensors for the construction and control of biosynthetic pathways. *Metab. Eng. 14*, 212−222.
(29) Schallmey, M., Frunzke, J., Eggeling, L., and Marienhagen, J. (2014) Looking for the pick of the bunch: high-throughput screening of producing microorganisms with biosensors. *Curr. Opin. Biotechnol. 26*, 148−154.
(30) Zhang, F., Carothers, J. M., and Keasling, J. D. (2012) Design of a dynamic sensor-regulator system for production of chemicals and fuels derived from fatty acids. *Nat. Biotechnol. 30*, 354−359.
(31) Xu, P., Li, L., Zhang, F., Stephanopoulos, G., and Koffas, M. (2014) Improving fatty acids production by engineering dynamic pathway regulation and metabolic control. *Proc. Natl. Acad. Sci. U. S. A. 111*, 11299−11304.
(32) Uchiyama, T., and Miyazaki, K. (2010) Product-induced gene expression, a product-responsive reporter assay used to screen metagenomic libraries for enzyme-encoding genes. *Appl. Environ. Microbiol. 76*, 7029−7035.
(33) Yamamoto, K., and Ishihama, A. (2005) Transcriptional response of *Escherichia coli* to external copper. *Mol. Microbiol. 56*, 215−27.
(34) Reese, M. G. (2001) Application of a time-delay neural network to promoter annotation in the Drosophila melanogaster genome. *Comput. Chem. 26*, 51−56.
(35) Rademacher, C., and Masepohl, B. (2012) Copper-responsive gene regulation in bacteria. *Microbiology 158*, 2451−2464.
(36) Munson, G. P., Lam, D. L., Outten, F. W., and O'Halloran, T. V. (2000) Identification of a copper-responsive two-component system on the chromosome of *Escherichia coli* K-12. *J. Bacteriol. 182*, 5864−5871.
(37) Mustafi, N., Grunberger, A., Kohlheyer, D., Bott, M., and Frunzke, J. (2012) The development and application of a single-cell biosensor for the detection of l-methionine and branched-chain amino acids. *Metab. Eng. 14*, 449−457.
(38) Thomason, L., Court, D. L., Bubunenko, M., Constantino, N., Wilson, H., Datta, S., and Oppenheim, A. (2005) Recombineering: genetic engineering in bacteria using homologous recombination. In *Current Protocols in Molecular Biology* (Ausubel, F. M., Brent, R., Klingston, R. E., Moore, D. D., Deidman, J. G., Smith, J. A., and Struhl, K., Ed.), pp 1.16.1−1.16.21, Wiley, NY.
(39) Sambrook, J., and Russell, R. W. (2001) *Molecular Cloning: A Laboratory Manual*, 3rd ed., Cold Spring Harbor Laboratory Press, Cold Spring Harbor, NY.
(40) Li, B., and Dewey, C. N. (2011) RSEM: accurate transcript quantification from RNA-Seq data with or without a reference genome. *BMC Bioinf. 12*, 323.
(41) He, L., Zhang, A., Pei, Y., Chu, P., Li, Y., Huang, R., Liao, L., Zhu, Z., and Wang, Y. (2017) Differences in responses of grass carp to different types of grass carp reovirus (GCRV) and the mechanism of hemorrhage revealed by transcriptome sequencing. *BMC Genomics 18*, 452−466.
(42) Kubista, M., Andrade, J. M., Bengtsson, M., Forootan, A., Jonak, J., Lind, K., Sindelka, R., Sjoback, R., Sjogreen, B., Strombom, L., Stahlberg, A., and Zoric, N. (2006) The real-time polymerase chain reaction. *Mol. Aspects Med. 27*, 95−125.
(43) Livak, K. J., and Schmittgen, T. D. (2001) Analysis of relative gene expression data using real-time quantitative PCR and the 2(-Delta Delta C(T)) Method. *Methods 25*, 402−408.

DOI: 10.1021/acssynbio.8b00317
ACS Synth. Biol. 2019, 8, 297−306